The thermoelectric properties of In_2O_3 thin films deposited by direct current magnetron sputtering

Fan Ye*, Xiao-Qiang Su, Xing-Min Cai, Huan Wang, Zhuang-Hao Zheng, Guang-Xing Liang, Ping Fan, Dong-Ping Zhang, Jing-Ting Luo

School of Physical Science and Technology and Shenzhen Key Laboratory of Sensor Technology, Shenzhen University, Shenzhen, 518060, China

*yefan@szu.edu.cn

Keywords: thin film; In_2O_3; thermoelectric; sputtering

Abstract In_2O_3 films were deposited on K9 glass by direct current magnetron sputtering with different oxygen partial pressure percentage. It is found that the films have a body-centered cubic structure, a relatively high transmission in the visible range and an optical band gap of around 3.75 eV. The conductivity of the films increases with the temperature increase up to around 470K due to the increase in the carrier concentration and then decreases due to scattering. The films are n-type and the absolute value of the Seebeck coefficient increases nearly linearly with the increase in the test temperature. The power factor of the films also roughly increases with the increase in the test temperature. It is found that oxygen partial pressure percentage has an effect on defects, electron density and Fermi level position. The films deposited with the oxygen partial pressure percentage of 80% have the best thermoelectric properties.

Introduction

Thermoelectric materials can be potentially used in power generation, solid state cooling and waste-heat recycle and therefore have recently attracted much attention [1-21] etc. In_2O_3 is a very important semiconductor since In_2O_3 doped with Sn is widely used as transparent electrodes in electronic devices[22]. There is some theoretical [13] and experimental work about the thermoelectric properties of In_2O_3 and its dopants [2, 5-18] . There is work [5-10] about In_2O_3 bulk and its dopant. For example, J. Lan et al. studied the thermoelectric properties of In_2O_3 codoped with Zn and Ge [5]. J. H. W. De Wit et al studied the thermoelectric power of In_2O_3 bulk [6]. M. Ohtaki et al. studied the high temperature thermoelectric properties of In_2O_3-based mixed oxides and the applicability to power generation [7]. There is also some work about In_2O_3 thin film and its dopant [2, 11-18]. For example, V. Brinzari [2], S.R. Sarath Kumar [17] and C.-Y. Wu [18] et al. studied the thermoelectric properties of In_2O_3 films doped with Sn. M. Liess et al. [14] used the thermoelectric properties of In_2O_3 film to fabricate a sensor based on the junction of In_2O_3 film and gold. L. C. Jimenez B et al.[15] studied the thermoelectric properties of In_2O_3 films below 400K. S.R. Sarah Kumar et al. [16] studied the role of oxygen vacancies in the high temperature thermopower of In_2O_3 in Ar ambient. The thermoelectric properties of In_2O_3 films and its dopant doped with S [11] or Pd [12] were also studied. Though doping might improve the thermoelectric properties of In_2O_3, much of the thermoelectric properties of undoped In_2O_3 has not been studied. For In_2O_3 films deposited by sputtering, there is no report about the influence of oxygen partial pressure percentage on the thermoelectric properties of In_2O_3 thin films deposited with high oxygen partial pressure. Therefore, we fabricated In_2O_3 thin films by DC magnetron sputtering with different oxygen partial pressure percentage and studied their thermoelectric properties.

Experiments

In_2O_3 films were fabricated by reactive DC magnetron sputtering (JGP 450, SKY Technology Development Corporation Limited, Chinese Academy of Sciences) under different gas flow rates. The substrates were K9 glass which had been ultrasonically washed in acetone, ethanol and de-ionized

water. The washing in each liquid was 15 minutes. The sputtering chamber was pumped to 6.0×10^{-4} Pa before deposition. The target was a metallic indium (In) disk (99.999%). Three batches of samples were fabricated. The flow rate of O_2 was always 40 standard cubic centi-meters per minute (sccm) while the flow rate of Ar was 0, 10 and 26.7 sccm respectively. Correspondingly, the O_2 partial pressure percentage (P_{O_2}) was 100%, 80% and 60% when the flow rate of Ar was 0, 10 and 26.7 sccm. The sputtering pressure was always 5.0×10^{-1}Pa for the three batches of samples. During deposition, the substrate temperature was 350 ℃ and the substrates were rotated at 13.8 revolutions per minute (rpm). The sputtering current and voltage were 0.08 A and 0.28 kV. The deposition time for each batch of samples was 30 minutes.

The thickness of the samples was measured by a surface profiler (Veeco Dektak 3ST) and the thicknesses of the samples deposited with an Ar flow rate of 0, 10 and 26.7 sccm were 150, 106 and 115 nm respectively. The crystal structure of the samples was studied with X-ray diffraction (XRD, D/max 2500 PC, maximum power 18 kW, Cu Kα radiation). A UV/VIS spectrophotometer (Perkin-Elmer, Lambda 900) was used to measure the transmission and reflection of the samples and an integrating sphere was used for the reflection measurements. The electrical conductivity of the samples was measured using the four-probe technique (Keithley 400). The Seebeck coefficient was measured with a home-made thin-film Seebeck measurement system and the temperature gradient method (ΔV/ΔT) was used. The electromotive force (ΔV) and temperature gradient (ΔT) were measured by a couple of copper probes and thermocouples at the same positions of the samples.

Results and discussion

The XRD patterns of all the samples are shown in Fig.1. For the three batches of samples, the only diffraction peak was located at 30.24P^{o} and no other peaks were found. This is different from In_2O_3 films prepared by spray pyrolysis where many more peaks were observed [11]. The peak at 30.24^{o} was due to the (222) reflection of body centered cubic (bcc) In_2O_3 [11, 23, 24]. All the samples have a preferred (111) orientation. The (111) preferred orientation was also observed in pulsed-laser-deposited In_2O_3 with GaAs as the substrate [23]. The XRD results are in agreement with those for p-type In_2O_3 deposited on quartz glass by DC sputtering [25]. According to the XRD data and Scherer formula [11], the grain size of the three samples is estimated to be 14.20 nm.

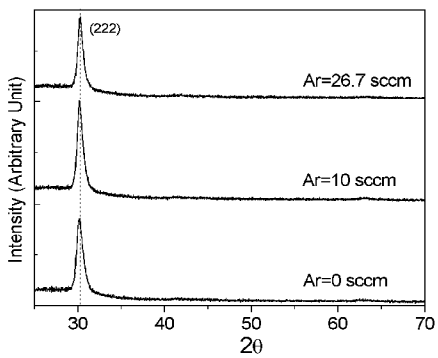

Figure 1 X-Ray diffraction patterns of the films.

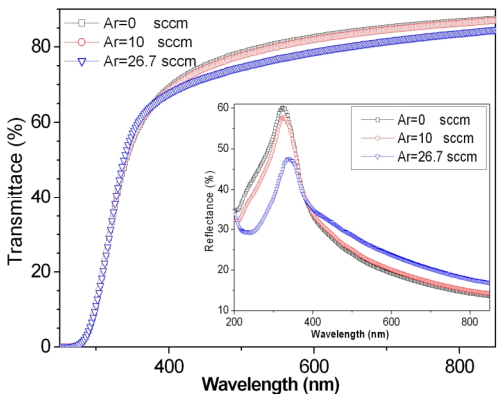

Figure 2 Transmittance spectra of the films. The insetshows the diffuse reflectance spectra of the films.

The transmittance and diffuse reflectance spectra of all the samples are shown in Fig.2. It can be found that below 400 nm, lower oxygen partial pressure ratio leads to similar transmittance and lower reflectance, while over 400 nm lower oxygen partial pressure ratio leads to lower transmittance and higher reflectance. This results from different atomic ratios of In to O since lower oxygen partial pressure ratio will increase the atomic ratios of In to O in the films. The transmittance spectra of all the

samples are similar to those of In_2O_3 deposited by reactive evaporation of In in an oxygen atmosphere [26] or spray pyrolysis [11]. The diffuse reflectance spectra of all the samples are similar to those of GaO_3- In_2O_3-SnO_2 systems [27]. The samples have relatively high transmittance in the range of visible spectra. If both the air/film interface and film/glass interface are assumed to have the same reflectance R, the absorption coefficient a can be induced from the reflectance R, transmittance T and the film thickness [28]. Based on the relation between a , photon energy $h\upsilon$ and the optical band gap E_g and Tauc plot, the optical band gap E_g of all the samples are found to be 3.75 eV. These values are roughly in accordance with the onset of strong optical absorption of single crystalline bcc In_2O_3 [29] but smaller than those prepared by spray pyrolysis [11].

Figure 3 shows the dependence of the conductivity on the temperature. The conductivity s can be written as $s = nem$ where n is the density of electrons, e the charge of an electron and m the electron mobility since Seebeck tests show that all the samples are n-type. With the increase in the temperature, the conductivity first increases and then decreases. Around 470K, the samples show the highest conductivity. Though the In_2O_3 films were not intentionally doped, their conductivity is different from intrinsic semiconductors whose conductivity increases monotonically with the increase in the temperature. This is because there are defects in unintentionally doped In_2O_3. These defects include vacancies and interstitials. Oxygen vacancies (V_O) and interstitial indium (In_i) are donors in In_2O_3 while interstitial oxygen (O_i) and indium vacancies (V_{In}) are acceptors in In_2O_3 [30,31]. These defects play the role of impurities, which makes the behavior of our unintentionally doped In_2O_3 similar to that of doped In_2O_3. With the temperature increase up to about 470K, more donors are excited and the density of electrons increases, which leads to the increase in the conductivity s with the temperature increase up to about 470K. The decrease in the conductivity s over 470K is possibly due to the decrease in the electron mobility which results from strong scattering generated by lattice vibration or grain boundary scattering. The resistivity of co-sputtering deposited In_2O_3 increases with the increase in the temperature till the temperature is around 900K [12]. The difference between the samples deposited by co-sputtering and ours might result from different fabrication methods.

Figure 4 shows the dependence of the Seebeck coefficient S of all the samples on the temperature. Since all the samples have negative Seebeck coefficients, the samples are all n-type. At 520K, the Seebeck coefficient of the samples deposited with an Ar flow rate of 10 and 26.7 sccm is about -200 μV/K and the absolute value is larger than that of the sample deposited without Ar. The absolute value of Seebeck coefficient S increases with the increase in the range of the test temperature. The temperature dependence of the Seebeck coefficient of our samples roughly agrees with those of unintentionally doped In_2O_3 bulk [6] and In_2O_3:Pd nanocomposite films [12], but disagrees with others [10, 11], due to different range of test temperatures or different fabrication methods. Our films were sputtering deposited with a grain size of 14.20 nm as calculated and they are not granular materials [19-21] since films deposited by sputtering are usually dense enough and the grains inside the films are in close contact with each other. For a degenerate semiconductor with parabolic bands, the relation between the Seebeck coefficient S and the temperature T is

$$S = -(p^2 k_B / e)(k_B T / E_F)(\frac{1}{2} - \frac{1}{3} r) \quad (1)$$

where k_B is the Boltzmann constant, E_F is the Fermi energy and r is the scattering index [16]. If we assume that E_F and r are temperature-independent, S will change linearly with the temperature T. For the samples prepared with an Ar flow rate of 0 sccm (P_{O_2} of 100%) and 10 sccm (P_{O_2} of 80%), the relation between S and T is roughly linear. This linearity possibly suggests that In_2O_3 films have a high Debye temperature and a free-electron-like energy band structure with a small phonon-drag term [18]. From the above formula, it can also be found that the absolute value of the slope of the S~T curve is inverse to E_F and therefore the samples deposited with the O_2 partial pressure of 80% have the lowest E_F and the lowest electron density with the assumption that all the samples have the same density of

states. The low electron density will lead to low conductivity if it is assumed that all have the same mobility. A combination of Fig.3 and Fig.4 suggests that both high and low O_2 partial pressure percentage (such as 100% and 60%) favor the formation of donor-type defects. For the samples prepared with an Ar flow rate of 26.7 sccm (P_{O_2} of 60%), the linear relation between S and T has a transition at around 500 K and the reason needs further study. Why S does not approach zero with T approaching zero for the samples prepared with an Ar flow rate of 10 sccm (P_{O_2} of 80%) also needs further study.

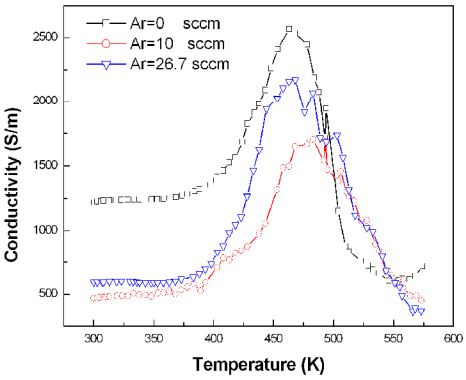

Figure 3 The dependence of the conductivity of the films on the temperature.

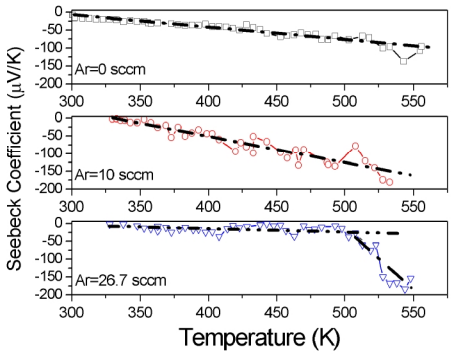

Figure 4 The dependence of the Seebeck coefficient of the films on the temperature. The square, circle and triangle denote the data points while the dash and dot lines are linearly fitted according the data points.

The power factor of thermoelectric materials is defined by $S^2 s$ where S is the Seebeck coefficient and s is the conductivity. Fig.5 shows the temperature dependence of the power factors of all the samples. For the samples deposited with an Ar flow rate of 0 sccm (P_{O_2} of 100%) and 10 sccm (P_{O_2} of 80%), the power factor shows a relatively fast increase at around 400K, while for the samples deposited with an Ar flow rate of 26.7 sccm (P_{O_2} of 60%), the power factor hardly increases with the increase in the temperature. Among all the samples, the samples deposited with P_{O_2} of 80% has the maximum power factor of 30 $\mu Wm^{-1}K^{-2}$ around 520K and it is almost three times that of the samples deposited with P_{O_2} of 100% and 60%, implying that the O_2 partial pressure has a great effect on the thermoelectric properties.

The power factors of our samples roughly increase with the increase in the temperature, which is similar to those of undoped In_2O_3 and Pd doped In_2O_3 films [12] or undoped In_2O_3 and Co doped In_2O_3 bulk [10]. The power factors of our samples are slightly smaller than those of undoped In_2O_3 [12] at the same temperature, possibly due to different fabrication methods. At the same temperature, the power factors of our undoped In_2O_3 films are smaller than tin doped In_2O_3 films [2] and cobalt doped In_2O_3 bulk [10], suggesting that doping In_2O_3 with tin or cobalt can improve the power factors. Comparing Fig.4 and Fig.5, we can find that both the Seebeck coefficient S and the power factor $S^2 s$ possess a similar behavior with the increase in the temperature. This implies that with the increase in the temperature, the increase in the squared Seebeck coefficient S^2 is much greater and almost cancels the decrease in the conductivity s when the temperature is around or over 470K.

The figure of merit (zT) is defined by

$$zT = S^2 s T / k \quad (2),$$

where S^2s is the power factor, T is the temperature and k is the thermal conductivity [32]. If the thermal conductivity of phonons is ignored, k will be only from electrons and equal to LsT where L is the Lorenz factor (2.4×10^{-8} $J^2K^{-2}C^{-2}$) [32]. In this case, zT will be S^2/L and proportional to S^2. With the assumption that this model is also true for our samples and with the data from Fig.4, zT of the films deposited with P_{O_2} of 80% will be around 1.7 at 520K.

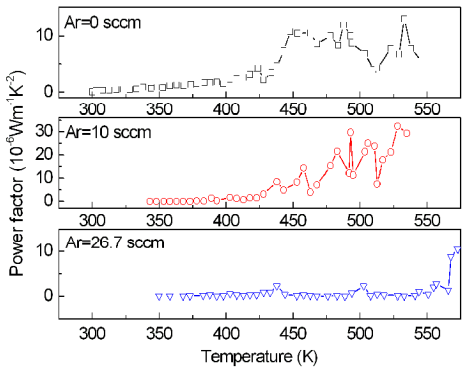

Figure 5 The dependence of the power factors of the films on the temperature.

Conclusion

We used direct current magnetron sputtering to deposit In_2O_3 films with different oxygen partial pressure percentage and studied their thermoelectric properties. XRD shows that the crystal structure of the films is body-centered cubic and all the films have a preferred orientation of (111). The visible range transmission of the samples is around 75% and the optical band gap was calculated to be around 3.75eV. In the range of the temperature measured, the conductivity of the films increases with the temperature increase, reaches the maximum at about 470K due to the increase in the electron density and then decreases due to increased scattering. Seebeck effect shows that all the samples are n-type and the absolute value of the Seebeck coefficient increases with the increase in the temperature. The power factors of the films also increase with the increase in the temperature. It is found that high oxygen partial (such as P_{O_2} of 100%) or low oxygen partial (such as P_{O_2} of 60%) will lead to the increase in the donor-type defects and the Fermi level, which will weaken the power factor and the value of the figure of merit. The films deposited with P_{O_2} of 80% are found to have the best thermoelectric properties. At 520K, the films deposited with P_{O_2} of 80% have a Seebeck coefficient of -200 μV/K, the maximum power factor of 30 $\mu Wm^{-1}K^{-2}$ and zT of 1.7 based on the assumption that the thermal conductivity is only from electrons.

Acknowledgement

This work was financially supported by National Natural Science Foundation of China (No.:61204010), Shenzhen City R&D funding for Science and Technologies—Basic Research Programs (No.: JCYJ20120613102126217 and JCYJ20120613172752576) and Shenzhen City Science and Technology Plan for Cooperation Innovation-The Matching Funding for National and Provincial Funding (20130301110056).

References

[1] C. X. Quintela, B. Rodríguez-González and F. Rivadulla, Appl. Phys. Lett. 104 (2014) 022103-1-022103-5.

[2] V. Brinzari, I. Damaskin, L. Trakhtenbergc, B. K. Cho, G. Korotcenkov, Thin Solid Films 552 (2014) 225-231.
[3] M. Ardyanian, M. Moeini, H. Azimmi Juybari, Thin Solid Films, 552 (2014) 39-45.
[4] R. Santos, J. Loureiro, A. Nogueira, E. Elangovan, J.V. Pinto, J.P. Veiga, T. Busani, E. Fortunato, R. Martins, I. Ferreira, Appl. Surf. Sci., 282 (2013) 590-594.
[5] J. Lan, Y.H. Lin, Y. Liu, S. Xu, C.-W. Nan, J. Am. Ceram. Soc. 95 (2012) 2465-2469.
[6] J.H.W. De Wit, J. Van Der Bom, J.F. De Groot, J. Solid State Chem. 25 (1978) 101-105.
[7] M. Ohtaki, D. Ogura, K. Eguchi and H. Arai, J. Mater. Chem. 4 (1994) 653-656.
[8] D. Bérardan, E. Guilmeau, A. Maignan and B. Raveau, Solid State Commun. 146 (2008) 97-101.
[9] E. Guilmeau, D. Bérardan, Ch. Simon, A. Maigana, B. Raveau, D. Ovono Ovono and F. Delorme, J. Appl. Phys. 106 (2009) 053715-1-053715-7.
[10] Y. Liu, Y.-H. Lin, J. Lan, W. Xu, B. P. Zhang, C.-W. Nan and H. Zhu, J. Am. Ceram. Soc. 93 (2010) 2938-2941.
[11] M. Hasan Zadeh Maha, M.-M. Bagheri-Mohagheghi, H. Azimi-Juybari, M. Shokooh-Saremi, Phys. Scr. 86 (2012) 055701-1-055701-7.
[12] O. J. Gregory, M. Amani, G. C. Fralick, Appl. Phys. Lett. 99 (2011) 013107-1-013107-3.
[13] S. M. Hosseini, H. A. Rahnamaye Aliabad, A. Kompany, Mod. Phys. Lett. 21 (2010) 2251-2265.
[14] M. Liess and H. Steffes, J. Electrochem. Soc. 147 (8) (2000) 3151-3153.
[15] Luis C. Jimenez B., Henry A. Méndez P., Beynor A. Páez S., María E. Ramírez O., Hernán Rodríguez H., Brazilian J. Phys. 36 (2006) 1017-1020.
[16] S.R.Sarath Kumar and S. Kasiviswanathan, Semicond. Sci. Technol. 24 (2009) 025028-1-025028-7.
[17] S.R. Sarath Kumar, V. Damodara Das, S. Kasiviswanathan, Thin Solid Films 518 (2009) 1390-1393.
[18] C.-Y. Wu, T. V. Thanh, Y.-F. Chen, J.-K. Lee and J.-J. Lin, J. Appl. Phys. 108 (2010) 123708-1-123708-3.
[19] I. S. Beloborodov, A. V. Lopatin, V. M. Vinokur, and K. B. Efetov, Rev. Mod. Phys. 79 (2007) 469-518.
[20] A. Glatz and I. S. Beloborodov, Europhys. Lett.87 (2009) 57009-1-57009-4.
[21] A. Glatz and I. S. Beloborodov, Phys. Rev. B 80 (2009) 245440-1-245440-4.
[22] I. Hamberg, C. G. Granqvist, J. Appl. Phys. 60 (1986) R123-R159.
[23] N. Tripathia, S. Rath, V. Ganesan, R. J. Choudhary, Appl. Surf. Sci. 256 (2010) 7091-7095.
[24] Joint Committee on Powder Diffraction, Standards-International Center for Diffraction Data Card No.89-4595.
[25] J. Stankiewicz, F. Villuendas, R. Alcalá, Appl. Phys. Lett. 96 (2010) 192108-1-192108-3.
[26] E. B. Ali, H. E. Maliki, J. C. Bernede , M. Sahnoun, A. Khelil, O. Saadane, Mater. Chem. Phys. 73 (2002) 78-85.
[27] D. D. Edwards, T. O. Mason, F. Goutenoire, K. R. Poeppelmeier, Appl. Phys. Lett. 70 (1997) 1706-1708.
[28] K. J. Lethy, D. Beena, V. P. M. Pillai, V. Ganesan, J. Appl. Phys**.** 104 (2008) 033515-1-033515-12**.**
[29] C. Y. Wang, V. Cimalla, H. Romanus, T. Kups, G. Ecke, T. Stauden, M. Ali, V. Lebedev, J. Pezoldt, O. Ambacher, Appl. Phys. Lett. 89 (2006) 011904-1-011904-3.
[30] P. Reunchan , X. Zhou, S. Limpijumnong, A. Janotti, C. G. V. de Walle, Curr. Appl. Phys. 11 (2011) S296-S300.
[31] L. M. Huang, C. Arhammar, C. M. Araújo, F. Silvearv, R. Ahuja, Europhys. Lett. 89 (2010) 47005-1-47005-5.
[32] G. J. Snyder, E. S. Toberer, Nature Mater. **7 (**2008**)** 105-114.